Sigma Journal of Engineering and Natural Sciences
Web page info: https://sigma.yildiz.edu.tr
DOI: 10.14744/sigma.2026.2061

Research Article

A numerical investigation for solving the sir model of covid 19 spread in Türkiye

Demet ÖZDEK[1,*]

[1]*Department of Mathematics, Izmir University of Economics, Izmir, 35330, Türkiye*

ARTICLE INFO

Article history
Received 04 September 2024
Revised 23 October 2024
Accepted 27 March 2025

Keywords:
SIR Model, Covid 19 Spread, Chebyshev Polynomials, Legendre Polynomials, Laguerre Polynomials

ABSTRACT

With the emergence of Covid 19, researchers have begun to address the spread of the disease from various perspectives. Some researchers have focused on statistical analysis to model these problems by fitting the data set or performing stability analysis to construct a theoretical framework for the solutions of these mathematical models. After all, they finalized their studies using a numerical technique to confirm that the model accurately depicts how the disease progresses. For this purpose, Runge Kutta methods are widely used in the literature as numerical techniques, because of their easy implementation. However, these methods do not explicitly provide approximate solutions for problems with no exact solution; thus, their accuracy cannot be discussed through error analysis. Therefore, this study deals with a numerical investigation to find approximate solutions of the Susceptible-Infected-Removed model for Covid 19 spread in Türkiye, using Chebyshev, Legendre and Laguerre polynomials. These polynomials can be easily implemented without the need for discretization and are effective in solving systems of nonlinear ordinary differential equations. The main idea of the method used in this study is to approximate the solution and its derivatives using a truncated series of orthogonal polynomials and convert the differential equation system into an algebraic equation system. Then, the obtained system is solved using MATLAB for unknown coefficients, which results in an approximate solution. To demonstrate the implementation of the method, the model is considered with official data regarding the course of Covid 19 in Türkiye. The obtained approximate solutions are compared with the other numerical results in figures and tables, and highly accurate results are obtained such as absolute errors and residual errors being around 10^{-10}. Therefore, this method, based on orthogonal polynomials, can be adopted to address more challenging real-life problems.

Cite this article as: Özdek D. A numerical investigation for solving the sir model of covid 19 spread in Türkiye. Sigma J Eng Nat Sci 2026;44(3):1754−1767.

INTRODUCTION

Throughout history, many pandemics such as Plague, Cholera, Influenza, Human Immunodeficiency Virus (HIV), Ebola have occurred that threaten human health and cause the death of millions of people. These pandemics have affected not only the health system and pharmaceutical industry, but also the economy, and have had

***Corresponding author.**
*E-mail address: demet.ersoy@ieu.edu.tr

This paper was recommended for publication in revised form by Editor-in-Chief Ahmet Selim Dalkilic

Published by Yıldız Technical University Press, İstanbul, Turkey

devastating impacts on politics, education, and social life, forcing governments to face very difficult situations [1-3]. Thus, the spread of pandemics has been of great concern to every individual for years.

In the 21st century, in December 2019, a novel coronavirus (SARS-CoV-2) causing pneumonia-like cases was identified in Wuhan City, Hubei Province, China. Subsequently, it was concluded that this disease led to a severe and potentially fatal respiratory syndrome. The disease spread rapidly around the world was declared as Covid 19 pandemic by the World Health Organization (WHO). Due to the lack of proper medicine or vaccines, in order for countries to overcome the pandemic, the WHO published guidelines on its website and governments have taken a series of precautions such as quarantine of suspected individuals, wearing masks, social distancing, self-isolation, and lock down, to control the spread of the disease [3]. While every individual made an effort to fight the pandemic that affected every aspect of society, researchers have directed their studies to understand the dynamic pattern of the disease [4-6]. In this sense, the mathematical models for epidemic diseases make contributions that provide a way to determine the course of the pandemic.

The literature on the system of differential equations describing a physical phenomenon or biological process consists of both theoretical and numerical results. Theoretical studies focus on the statistical analysis of the problem parameters that fit the model or stability analysis of the solutions for the problem. On the other hand, numerical investigations present approximate solutions that are valuable in the absence of exact solutions and support theoretical studies with error analysis of the solutions. As the approximate solutions of an epidemic model can be used for comparison purposes, they can also present time-dependent simulations to determine the dynamics of the model and the model parameters that affect the most on healing process. Additionally, through error analysis, approximate solutions provide information about the accuracy that is crucial to observe the course of the disease and determine the recovery strategies accurately.

On the other hand, the accuracy of the approximate solutions relies on not only the efficiency of the numerical technique but also on the stability of model parameters. In other words, these models require real and reliable data to obtain accurate results. However, it is not always possible to obtain the reliable data. For this reason, among epidemic models, one of the most preferred model is the susceptible-infected-removed (SIR) model, since it requires limited data, due to its basic structure. As an epidemic model, SIR model divides the population into three compartments: the susceptible, infected and removed compartments and explains the transmission of the disease through these compartments, including only two model parameters: the transmission rate and recovery rate. Many other epidemic models are derived from the SIR model. This means, when a numerical approach, applied on SIR model, results in accurate solutions, then it can be adopted to solve more extended epidemic models. In this sense, the SIR epidemic model has attracted the interest of the researchers.

The literature on the SIR model mostly consists of stability analysis or other qualitative features of the model.

Numerical techniques in these studies have only been tackled to confirm their theoretical results [7-19]. In this sense, Runge-Kutta methods are mostly used for this purpose, however these methods do not explicitly provide approximate solutions for problems with no exact solution; therefore, the accuracy cannot be discussed through error analysis.

There are only a few papers devoted to finding approximate solutions of the model for Covid 19 spread. In [20], Türkyilmazoğlu obtained numerical and non-numerical solutions to SIR and SEIR epidemic models, in form of exponential series. In [21], Prodanov derived a double exponential analytical asymptotic solution for the I-variable to use in parametric estimation. In [22], Barlow and Weinstein obtained a closed-form solution of the SIR model for the Covid 19 spread by the use of asymptotic approximants. Hasan et al. [23] used a generalized Taylor series-based method to solve the SIR epidemic model of fractional order and obtained an approximate solution in terms of convergent power series. Polynomial-based collocation methods are among the preferred methods for numerically solving the SIR model of the Covid 19 spread. For instance, Hermite polynomial solutions for the SIR model of Covid 19 were derived in [24]. Uçar and Çelik obtained approximate solutions using the Taylor Matrix method [25]. A Taylor wavelet-based numerical algorithm was used to obtain approximate solutions in [26]. Shiralashetti and Kumbinarasaiah used a numerical method based on Laguerre wavelets to solve the SIR epidemic model [27]. The approximate solutions of the SIR model for the Covid 19 spread are obtained by a collocation method based on the Chebyshev Polynomials in [28] and the Pell-Lucas collocation method in [29]. More recently, Gegenbauer wavelet solutions of the SIR and SITR models for the Covid 19 spread were obtained as the approximate solutions of the models, and the effects of the problem parameters were discussed in [30].

This study focuses on finding approximate solutions for the SIR epidemic model of the transmission of Covid 19 in Türkiye using a numerical technique based on orthogonal polynomials and presents their comparisons with each other and with the previous appropriate ones as a numerical investigation. It is known that exact solutions of realistic systems either cannot be found or are difficult to find. Thus, the approximate solutions of these systems are essential to the literature. On the other hand, the most accurate approximate solutions can give the most reliable information about the determination of the disease dynamics. Therefore, we aim to present approximate solutions of the SIR model for Covid 19 using different orthogonal polynomials such as the Chebyshev polynomial method (CPM), Legendre polynomial method (LePM) and Laguerre polynomial method (LaPM). The accuracy of their results are examined via error analysis to compare the abilities of the polynomials for solving the model.

As mentioned previously, in the epidemic SIR model, the total population is divided into three compartments: Susceptible, Infected and Removed populations. The susceptible population, denoted by $S(t)$, represents the individuals that are at risk of being infected after contact with the infected individuals, while the infected population, denoted by $I(t)$ represents the infected individuals and the removed population, denoted by $R(t)$ represents the individuals that are recovered and died from the Covid 19 disease. As an assumption of the SIR model, the total population $P = S + I + R$ remains constant. The flow of the population through the compartments is given by the following system of ordinary differential equations

$$\begin{aligned} \frac{dS(t)}{dt} &= -\frac{\beta}{P}S(t)I(t), \\ \frac{dI(t)}{dt} &= \frac{\beta}{P}S(t)I(t) - \nu I(t), \qquad 0 \le t \le L \qquad (1) \\ \frac{dR(t)}{dt} &= \nu I(t), \end{aligned}$$

$$S(0) = S_0,\ I(0) = I_0,\ R(0) = R_0 \qquad (2)$$

Here, L is the length of the interval, β is the transmission rate from susceptible individuals to infected individuals and ν is the rate of recovery from infected individuals to removed individuals.

The paper consists of three main sections named respectively as 'Structure of the Orthogonal Polynomials', 'Method of Solving' , 'Computational Experiments' and through these sections, this paper aims to

1. get approximate solutions of the SIR model for the spread of Covid 19, using the Chebyshev, Legendre and the Laguerre polynomials;
2. compare efficiency and the accuracy of the Chebsyhev polynomial method, Legendre polynomial method and Laguerre polynomial method for solving two examples of SIR model;
3. compare the results of mentioned methods with previous numerical techniques and each other.

Therefore the paper is organized as follows. In the section 'Structure of the Orthogonal Polynomials', we first introduce the structures of the Chebyshev, the Legendre and the Laguerre polynomials. In the section 'Method of Solving', the implementation of the method for solving SIR model is explained and then in the Section 'Computational Experiments', we demonstrate the implementation of the method on two examples. In the first example, the model is solved for comparison purposes; in the second example, the model is taken under consideration with official data regarding the course of Covid 19 in Türkiye. The obtained approximate solutions are compared with the numerical methods in figures and tables, and the accuracy of the method is examined through error analysis.

Structure of the Orthogonal Polynomials

The orthogonal set of polynomials consists of n-th degree polynomials $\{\phi_n(t)\}_{n=1}^{\infty}$ satisfying the orthogonality property on the interval $[a,b]$ [31].

$$\int_a^b \phi_n(t)\phi_m(t)W(t)dt=\gamma_n\delta_{nm} \qquad (3)$$

where γ_n is a real number, δ_{nm} is the Kronecker delta and $W(t)$ is the weight function. If the polynomials are divided by $\sqrt{\gamma_n}$, the orthogonal set will be orthonormal and constitute an orthonormal basis such that a function $f(t) \in L^2\,[a,b]$ can be written in terms of $\phi_n(t)$ ass

$$f(t)=\sum_{n=0}^{\infty} f_n\phi_n(t) \qquad (4)$$

where $f_n=\int_a^b f(t)\phi_n(t)w(t)dt$. If the series in Equation 4 is truncated, the truncated series $\sum_{n=0}^{N} f_n\phi_n(t)$ approximates a square integrable function $f(t)$ defined on the bounded domain $[a,b]$, as N tends to ∞ [32-35]. When the interval of interest is a different bounded interval, the orthogonal polynomials should be shifted to that interval under a transformation together with all other properties.

Chebyshev Polynomials

The first type of Chebyshev polynomials $T_n^*(t)$ can be defined by a useful trigonometric property and explicitly generated by the recurrence relation [36, 37]

$$T_{n+1}^*(t) = 2tT_n^*(t) - T_{n-1}^*(t), \quad n \ge 1$$

for n = 0,1,2,… with the values $T_0^*(t) = 1$ and $T_1^*(t) = t$. They are known as the very well-known orthogonal polynomials satisfying Equation 3 on [-1,1] where $W(t)=\frac{1}{\sqrt{1-t^2}}$, $\gamma_n = \pi$ if $n = 0$ and $\gamma_n = \pi / 2$ if $n \neq 0$. When the Chebyshev polynomials are shifted by $T_n(t) = T_n^*(\frac{2}{L}t - 1)$ to the interval $[0,L]$ the orthogonality property is transformed to the shifted form

$$\int_0^L T_n(t)T_m(t)w(t)dt = \frac{L}{2}\gamma_n\delta_{nm}\,,$$

with $w(t) = \mathrm{W}(\frac{2}{L}t - 1)$.

Legendre Polynomials

Legendre polynomials $P_n^*(t)$ can be derived from the recurrence relation [32, 34, 38]

$$P_{n+1}^*(t) = \frac{2n+1}{n+1}tP_n^*(t) - \frac{n}{n+1}P_{n-1}^*(t),\ n = 1,2,3, \ldots$$

with $P_0^*(t) = 1$ and $P_1^*(t) = t$. The orthogonality property in Equation 3 is satisfied by these polynomials over [-1,1] with respect to $W(t) = 1$, where $\gamma_n = \frac{2}{2n+1}$. The shifted Legendre polynomials $P_n(t) = P_n^*(\frac{2}{L}t - 1)$ satisfy the orthogonality property over $[0,L]$

$$\int_0^L P_n(t)P_m(t)w(t)dt = \frac{L}{2}\gamma_n\delta_{nm}.$$

Laguerre Polynomials

The polynomial solutions of the Laguerre Ordinary Differential Equation are known as Laguerre polynomials $L_n(t)$ which can be constructed in an explicit form [32, 39-43]

$$L_n(t) = \sum_{s=0}^{n}(-1)^s \frac{n!}{(n-s)!\,(s!)^2}t^s$$

or by the recurrence relation

$$L_{n+1}(t) = \frac{2n+1-t}{n+1}L_n(t) - \frac{n}{n+1}L_{n-1}(t), \quad n = 1,2,3,\ldots$$

with $L_0(t) = 1$ and $L_1(t) = t + 1$. The Laguerre polynomials are orthonormal over an unbounded interval $[0,\infty]$ with respect to the weight function $W(t) = e^{-t}$ and $\gamma_n = 1$. In this case, one can see the theorem in [44] such that the truncated series $\sum_{n=0}^{N} f_n L_n(t)$ converges uniformly to a function $f(t)$ defined on the unbounded domain $[0, \infty]$ as N tends to ∞, if the conditions of the theorem are satisfied.

METHOD OF SOLVING

In this section, we discuss the implementation of orthogonal polynomials in a general framework and, then adapt this numerical method to Chebyshev, Legendre and Laguerre polynomials to solve the SIR epidemic model of Covid 19. We assume that the solutions of the model in Equations 1 and 2 have the following form

$$\begin{aligned} S_N(t) &= \sum_{n=0}^{N} a_n\phi_n(t) = \boldsymbol{A}^T\boldsymbol{\psi}(t) \\ I_N(t) &= \sum_{n=0}^{N} b_n\phi_n(t) = \boldsymbol{B}^T\boldsymbol{\psi}(t) \\ R_N(t) &= \sum_{n=0}^{N} c_n\phi_n(t) = \boldsymbol{C}^T\boldsymbol{\psi}(t) \end{aligned} \tag{5}$$

where a_n, b_n and c_n are the unknown coefficients; $\phi_n(t)$ represents the relevant polynomial, that is, $\phi_n(t)$ is the shifted Chebyshev polynomial for $\phi_n(t) = T_n(t)$ or the shifted Legendre polynomial for $\phi_n(t) = P_n(t)$ or the Laguerre polynomial for $\phi_n(t) = L_n(t)$ for each $n = 0,1,2,\ldots,N$ and for a positive integer N, $\boldsymbol{A}$, $\boldsymbol{B}$, $\boldsymbol{C}$ and $\boldsymbol{\psi}(\boldsymbol{t})$ are $(N + 1) \times 1$ matrices of the form

$$\begin{aligned} \boldsymbol{A} &= [a_0\ a_1\ a_2\ \ldots\ a_{N-1}]^T, \\ \boldsymbol{B} &= [b_0\ b_1\ b_2 \ldots b_{N-1}]^T, \\ \boldsymbol{C} &= [c_0\ c_1\ c_2\ \ldots\ c_{N-1}]^T, \\ \boldsymbol{\psi}(\boldsymbol{t}) &= [\phi_0(t)\ \phi_1(t) \ldots \phi_{N-1}(t)]^T. \end{aligned} \tag{6}$$

To obtain unknown coefficients a_n, b_n and c_n, $n = 0,1,2,\ldots,N$ we first represent the derivatives of the solutions $S_N(t)$, $I_N(t)$, $R_N(t)$ in matrix forms, utilizing the $(N + 1) \times (N + 1)$ operational differentiation matrix $\boldsymbol{D}$ given in Remark

$$\begin{aligned} S'_N(t) &= \textstyle\sum_{n=0}^{N-1} a_n\,\phi_n'(t) = \boldsymbol{A^T D\,\psi(t)}, \\ I'_N(t) &= \textstyle\sum_{n=0}^{N-1} b_n\,\phi_n'(t) = \boldsymbol{B^T D\,\psi(t)}, \\ R'_N(t) &= \textstyle\sum_{n=0}^{N-1} c_n\,\phi_n'(t) = \boldsymbol{C^T D\,\psi(t)}. \end{aligned} \tag{7}$$

Remark. Note that $(N + 1) \times (N + 1)$ operational matrices for differentiation $\boldsymbol{D}$ for the shifted Chebyshev polynomials $T_n(t)$, shifted Legendre polynomials $P_n(t)$ and Laguerre polynomials $L_n(t)$ are given respectively [45-47]

For $\phi_n(t) = T_n(t)$,

$$\boldsymbol{D} = [d_{rs}] = \frac{2}{L}\begin{cases} 2(r-1), & if\ (r-s)\ is\ odd\ and\ r > s > 1 \\ \sqrt{2}(r-1), & if\ (r-s)\ is\ odd\ and\ r > s = 1 \\ 0, & otherwise \end{cases} \tag{8}$$

For $\phi_n(t) = P_n(t)$,

$$\boldsymbol{D} = [d_{rs}] = \frac{2}{L}\begin{cases} 2(s-1),\ for\ s = r-\sigma, \\ \begin{cases} \sigma = 1,3,5,\ldots N, & if\ N\ is\ odd \\ \sigma = 1,3,5,\ldots N-1, & if\ N\ is\ even \end{cases} \\ 0, \qquad otherwise \end{cases} \tag{9}$$

$$\text{For } \phi_n(t) = L_n(t), \quad \boldsymbol{D} = [d_{rs}] = -\begin{cases} 1, & if\ r > s, \\ 0, & otherwise \end{cases} \tag{10}$$

Then we substitute $S_N(t)$, $I_N(t)$, $R_N(t)$ and their derivatives into Equations 1 and 2 to get

$$\begin{aligned} &\boldsymbol{A^T D\psi}(t) = -\frac{\beta}{P}\boldsymbol{A^T\psi}(t)[\boldsymbol{\psi}(t)]^T\boldsymbol{B} \\ &\boldsymbol{B^T D\psi}(t) = -\frac{\beta}{P}\boldsymbol{A^T\psi}(t)[\boldsymbol{\psi}(t)]^T\boldsymbol{B} - \nu\boldsymbol{B^T\psi}(t) \\ &\boldsymbol{C^T D\psi}(t) = \nu\boldsymbol{B^T\psi}(t) \\ &\boldsymbol{A^T\psi}(0) = S_0, \quad \boldsymbol{B^T\psi}(0) = I_0, \quad \boldsymbol{C^T\psi}(0) = R_0 \end{aligned}$$

Finally, in the obtained system above, the collocation points

$$t_i = \frac{L}{N-1}(i-1), \quad i = 1,2,\ldots,N$$

are replaced instead of t and together with the initial conditions, this yields a system of $3(N+1)$ equations

$$\begin{aligned} \boldsymbol{A^T D \psi(t_i)} &= -\frac{\beta}{P}\boldsymbol{A^T \psi(t_i)}[\boldsymbol{\psi(t_i)}]^T\boldsymbol{B} \\ \boldsymbol{B^T D \psi(t_i)} &= -\frac{\beta}{P}\boldsymbol{A^T \psi(t_i)}[\boldsymbol{\psi(t_i)}]^T\boldsymbol{B} - \nu \boldsymbol{B^T \psi(t_i)} \\ \boldsymbol{C^T D \psi(t_i)} &= \nu \boldsymbol{B^T \psi(t_i)} \end{aligned} \tag{11}$$

$$\boldsymbol{A^T\psi}(0) = S_0, \quad \boldsymbol{B^T\psi}(0) = I_0, \quad \boldsymbol{C^T\psi}(0) = R_0 \tag{12}$$

that can be solved for a_n, b_n and $c_n n = 0,1,2,\ldots, N$ using MATLAB. The obtained coefficients are replaced in the approximate solutions of the model in Equations 1 and 2, as follows

$$S_N(t) = \sum_{n=0}^{N} a_n\phi_n(t), \quad I_N(t) = \sum_{n=0}^{N} b_n\phi_n(t),$$
$$R_N(t) = \sum_{n=0}^{N} c_n\phi_n(t).$$

COMPUTATIONAL EXPERIMENTS

In this section, we demonstrate the adaptation of the method to the Chebyshev polynomials for solving the SIR epidemic model for transmission of Covid 19 and the adaptation to the Legendre and Laguerre polynomials can be performed in a similar way. We focus on two computational examples. In the first example, we solve the problem within the interval [0,1] for comparison purposes, by taking the parameter values and initial conditions from [26, 27]. After ensuring that the proposed method is efficient and has good accuracy, in the second example, we extend the interval to [0,60] and use the real reported data as initial conditions and the parameter values to observe the course of the disease in a two-month period.

Example 1. In this example, we consider the SIR epidemic model with transmission rate $\beta = 0.01$, recovery rate $\nu = 0.02$ and initial condition $S(0) = 20$, $I(0) = 15$, $R(0) = 10$. Setting $N = 7$, we assume that the solutions of the SIR epidemic model have the formm

$$\begin{aligned} S_7(t) &= \textstyle\sum_{n=0}^{7} a_n\phi_n(t) = \boldsymbol{A^T\psi}(t) \\ I_7(t) &= \textstyle\sum_{n=0}^{7} b_n\phi_n(t) = \boldsymbol{B^T\psi}(t) \\ R_7(t) &= \textstyle\sum_{n=0}^{7} c_n\phi_n(t) = \boldsymbol{C^T\psi}(t) \end{aligned} \tag{13}$$

where the interval is set as [0,1] for $L = 1$, $\psi(t)$, ***A, B, C*** are given in Equation 6, for $n = 0,1,2,\ldots,7$. Considering the 8×8 operational differentiation matrix for the shifted Chebyshev polynomials in the form

$$\boldsymbol{D} = 2\begin{bmatrix} 0 & 0 & 0 & 0 & 0 & 0 & 0 & 0 \\ \sqrt{2} & 0 & 0 & 0 & 0 & 0 & 0 & 0 \\ 0 & 4 & 0 & 0 & 0 & 0 & 0 & 0 \\ 3\sqrt{2} & 0 & 6 & 0 & 0 & 0 & 0 & 0 \\ 0 & 8 & 0 & 8 & 0 & 0 & 0 & 0 \\ 5\sqrt{2} & 0 & 10 & 0 & 10 & 0 & 0 & 0 \\ 0 & 12 & 0 & 12 & 0 & 12 & 0 & 0 \\ 7\sqrt{2} & 0 & 14 & 0 & 14 & 0 & 14 & 0 \end{bmatrix},$$

the derivatives of $S_7(t)$, $I_7(t)$, $R_7(t)$ can be represented by Equation 7. We substitute $S_7(t)$, $I_7(t)$, $R_7(t)$ and their derivatives into Equation 1; then, in place of t we write the collocation points

$$t_i = \frac{L}{N-1}(i-1), \quad i = 1,2,\ldots,7$$

to obtain 21 equations in the form of Equation 11. Together with the initial conditions

$$\boldsymbol{A^T\psi}(0) = 20, \quad \boldsymbol{B^T\psi}(0) = 15, \quad \boldsymbol{C^T\psi}(0) = 10,$$

we solve the system of 24 equations for the unknown coefficients a_n, b_n, c_n for $n = 0,1,2,\ldots,7$ using MATLAB to obtain the Chebyshev polynomial solutions. The instructions for finding approximate solutions is summarized as follows

Step 1. Input the values of the problem parameters β, ν, P and initial conditions S_0, I_0, R_0

Step 2. Choose N that corresponds to the degree of the polynomial approximations

Step 3. Construct the matrices ***AT, BT, CT, D, ψ***

Step 4. Enter the collocation points $t_i = \frac{L}{N-1}(i-1),\ i = 1,2,\ldots,N$

Step 5. Determine the system to solve for unknown coefficients

Step 6. Solve the system for unknown coefficients by aid of Matlab

Step 7. Replace the obtained coefficients in the truncated series

Step 8. Output the approximate solutions *S, I, R*

Following a similar process with the operational matrices of Legendre and Laguerre polynomials in Equations 9 and 10, we can construct the Legendre polynomial solutions and the Laguerre polynomial solutions. As a result, the Chebyshev polynomial solutions, the Legendre polynomial solutions and the Laguerre polynomial solutions are given in Table 1.

This example compares the accuracy and efficiency of the proposed methods with each other and previous numerical techniques in the literature. The model in this example has been previously solved by Taylor wavelet method (TWM) [26] and the Laguerre wavelet method (LaWM) [27]. In order to compare efficiency, we first compute the absolute errors of the obtained approximate solutions. Since the model does not have any analytic solution, we compare the absolute errors of the approximate solutions

Table 1. The chebyshev polynomial solutions, the legendre polynomial solutions and the laguerre polynomial solutions for $N = 7$

$S_9(t), I_9(t), R_9(t)$	a_n, b_n, c_n	$\phi_n(t)$		
		$\phi_n(t) = T_n(t)$ CPM	$\phi_n(t) = P_n(t)$ LePM	$\phi_n(t) = L_n(t)$ LaPM
$S_9(t) = \sum_{n=0}^{9} a_n \phi_n(t)$	a_0	32,77626653	32,77642486	30,13151082
	a_1	-1,89142261	-1,892097452	1,822821602
	a_2	-0,000335817	-0,000447561	0,068178022
	a_3	0,001124929	0,001800609	-0,018191218
	a_4	$-2{,}57378 \times 10^{-7}$	$-4{,}71467 \times 10^{-7}$	-0,000959939
	a_5	$-8{,}14144 \times 10^{-7}$	$-1{,}65487 \times 10^{-6}$	-0,002559686
	a_6	$5{,}4219 \times 10^{-10}$	$1{,}18895 \times 10^{-9}$	0,001364668
	a_7	$5{,}9938 \times 10^{-10}$	$1{,}43004 \times 10^{-9}$	-0,000193192
$I_9(t) = \sum_{n=0}^{9} b_n \phi_n(t)$	b_0	28,97580658	28,97763701	31,31339437
	b_1	1,686513301	1,687184258	-1,585532097
	b_2	-0,003883262	-0,005178944	-0,083253863
	b_3	-0,001118454	-0,001790248	0,017292524
	b_4	$1{,}65646 \times 10^{-6}$	$3{,}03047 \times 10^{-6}$	0,000988861
	b_5	$8{,}12486 \times 10^{-7}$	$1{,}6515 \times 10^{-6}$	0,002650748
	b_6	$-1{,}21965 \times 10^{-9}$	$-2{,}69058 \times 10^{-9}$	-0,001378344
	b_7	$-5{,}98509 \times 10^{-10}$	$-1{,}42797 \times 10^{-9}$	0,000192915
$R_9(t) = \sum_{n=0}^{9} c_n \phi_n(t)$	c_0	18,00835018	18,00636142	18,3155181
	c_1	0,20490931	0,204913194	-0,237289482
	c_2	0,004219079	0,005626505	0,015075774
	c_3	$-6{,}47486 \times 10^{-6}$	$-1{,}03613 \times 10^{-5}$	0,000898804
	c_4	$-1{,}39908 \times 10^{-6}$	$-2{,}559 \times 10^{-6}$	$-2{,}90279 \times 10^{-5}$
	c_5	$1{,}65768 \times 10^{-9}$	$3{,}36926 \times 10^{-9}$	$-9{,}10003 \times 10^{-5}$
	c_6	$6{,}7746 \times 10^{-10}$	$1{,}50163 \times 10^{-9}$	$1{,}36565 \times 10^{-5}$
	c_7	$-8{,}71178 \times 10^{-13}$	$-2{,}06968 \times 10^{-12}$	$2{,}79369 \times 10^{-7}$

of Chebyshev polynomials method (CPM), Legendre polynomials method (LePM), Laguerre polynomials method (LaPM), TWM and LaWM with the fourth-order Runge-Kutta method (RK4) with step size $\Delta t = 0.1$ in Table 2, assuming the Runge-Kutta solution as an exact solution. CPM, LePM and LaPM use 7th degree polynomials, while TWM and LaWM use respectively 10th and 8th degree polynomials. As shown in Table 2, all numerical methods achieve maximum absolute error around 10^{-9} for $S(t)$ and $I(t)$. For $V(t)$, CPM and LePM get maximum absolute error around 10^{-11}, LaPM and LaWM have maximum absolute error around 10^{-12} and the maximum absolute error of TWM is around 10^{-9} We can say that CPM, LePM and LaPM achieve similar absolute errors using lower degree polynomials. For this reason, CPM, LePM and LaPM.are as efficient as each other, but more efficient than TWM and LaWM.

In order to compare accuracy, we compute the absolute residual analysis ReS_N, ReI_N, ReR_N of CPM, LePM and LaPM by

$$ReS_N = \left| \frac{dS_N(t)}{dt} + \frac{\beta}{P} S_N(t) I_N(t) \right|,$$

$$ReI_N = \left| \frac{dI_N(t)}{dt} - \frac{\beta}{P} S_N(t) I_N(t) + \nu I_N(t) \right|,$$

$$ReR_N = \left| \frac{dR_N(t)}{dt} - \nu I_N(t) \right|.$$

In Table 3, the absolute residual errors of CPM, LePM and LaPM are compared with those of TWM but not with those of LaWM, because the absolute residual errors of the Laguerre wavelet solutions in [27] cannot be calculated. As can be seen in Table 3, the approximate solutions of CPM and LePM have better accuracy than LaPM with the same polynomial degree and achieve the same accuracy

Table 2. Comparison of the absolute errors of *CPM, LePM, LaPM, TWM* [26], *LaWM* [27] with *RK4* [created by author]

$S(t)$ $I(t)$ $R(t)$	t	*CPM* $N = 7$	*LePM* $N = 7$	*LaPM* $N = 7$	*TWM* [26] $N = 10$	*LaWM* [27] $N = 8$
	0	0	$6{,}9221 \times 10^{-11}$	$2{,}1284 \times 10^{-9}$	0	0
	0.1	$1{,}5295 \times 10^{-10}$	$8{,}4658 \times 10^{-11}$	$1{,}9649 \times 10^{-9}$	$1{,}5158 \times 10^{-10}$	$1{,}5154 \times 10^{-10}$
	0.2	$3{,}0144 \times 10^{-10}$	$2{,}3401 \times 10^{-10}$	$1{,}8033 \times 10^{-9}$	$2{,}9994 \times 10^{-10}$	$2{,}9941 \times 10^{-10}$
	0.3	$4{,}4753 \times 10^{-10}$	$3{,}8146 \times 10^{-10}$	$1{,}6427 \times 10^{-9}$	$4{,}4588 \times 10^{-10}$	$4{,}4532 \times 10^{-10}$
	0.4	$5{,}9173 \times 10^{-10}$	$5{,}3064 \times 10^{-10}$	$1{,}4801 \times 10^{-9}$	$5{,}9022 \times 10^{-10}$	$5{,}9021 \times 10^{-10}$
$S(t)$	0.5	$7{,}3495 \times 10^{-10}$	$6{,}9285 \times 10^{-10}$	$1{,}305 \times 10^{-9}$	$7{,}3379 \times 10^{-10}$	$7{,}3345 \times 10^{-10}$
	0.6	$8{,}79 \times 10^{-10}$	$8{,}9722 \times 10^{-10}$	$1{,}0895 \times 10^{-9}$	$8{,}7741 \times 10^{-10}$	$8{,}7674 \times 10^{-10}$
	0.7	$1{,}0236 \times 10^{-9}$	$1{,}2033 \times 10^{-9}$	$7{,}7467 \times 10^{-10}$	$1{,}0219 \times 10^{-9}$	$1{,}0217 \times 10^{-9}$
	0.8	$1{,}1681 \times 10^{-9}$	$1{,}7251 \times 10^{-9}$	$2{,}4438 \times 10^{-10}$	$1{,}168 \times 10^{-9}$	$1{,}1679 \times 10^{-9}$
	0.9	$1{,}3184 \times 10^{-9}$	$2{,}6681 \times 10^{-9}$	$7{,}1755 \times 10^{-10}$	$1{,}3166 \times 10^{-9}$	$1{,}316 \times 10^{-9}$
	1	$1{,}4786 \times 10^{-9}$	$4{,}3595 \times 10^{-9}$	$2{,}4648 \times 10^{-9}$	$1{,}4683 \times 10^{-9}$	$1{,}4676 \times 10^{-9}$
	0	0	$2{,}7125 \times 10^{-11}$	$8{,}4726 \times 10^{-10}$	0	0
	0.1	$1{,}5217 \times 10^{-10}$	$1{,}2568 \times 10^{-10}$	$6{,}7715 \times 10^{-10}$	$1{,}529 \times 10^{-10}$	$1{,}5286 \times 10^{-10}$
	0.2	$3{,}0064 \times 10^{-10}$	$2{,}7473 \times 10^{-10}$	$5{,}1 \times 10^{-10}$	$3{,}0172 \times 10^{-10}$	$3{,}01 \times 10^{-10}$
	0.3	$4{,}4686 \times 10^{-10}$	$4{,}2201 \times 10^{-10}$	$3{,}4429 \times 10^{-10}$	$4{,}4724 \times 10^{-10}$	$4{,}4669 \times 10^{-10}$
	0.4	$5{,}8967 \times 10^{-10}$	$5{,}6949 \times 10^{-10}$	$1{,}7826 \times 10^{-10}$	$5{,}9028 \times 10^{-10}$	$5{,}9027 \times 10^{-10}$
$I(t)$	0.5	$7{,}3045 \times 10^{-10}$	$7{,}2895 \times 10^{-10}$	$7{,}5673 \times 10^{-13}$	$7{,}3165 \times 10^{-10}$	$7{,}313 \times 10^{-10}$
	0.6	$8{,}7163 \times 10^{-10}$	$9{,}3007 \times 10^{-10}$	$2{,}1677 \times 10^{-10}$	$8{,}7217 \times 10^{-10}$	$8{,}7148 \times 10^{-10}$
	0.7	$1{,}0124 \times 10^{-9}$	$1{,}2317 \times 10^{-9}$	$5{,}3241 \times 10^{-10}$	$1{,}0126 \times 10^{-9}$	$1{,}0125 \times 10^{-9}$
	0.8	$1{,}1514 \times 10^{-9}$	$1{,}7469 \times 10^{-9}$	$1{,}0616 \times 10^{-9}$	$1{,}1539 \times 10^{-9}$	$1{,}1537 \times 10^{-9}$ s
	0.9	$1{,}2964 \times 10^{-9}$	$2{,}6824 \times 10^{-9}$	$2{,}0208 \times 10^{-9}$	$1{,}2967 \times 10^{-9}$	$1{,}2961 \times 10^{-9}$
	1	$1{,}4522 \times 10^{-9}$	$4{,}3648 \times 10^{-9}$	$3{,}7619 \times 10^{-9}$	$1{,}4419 \times 10^{-9}$	$1{,}4412 \times 10^{-9}$
	0	0	$2{,}5224 \times 10^{-13}$	$1{,}3127 \times 10^{-12}$	0	0
	0.1	$7{,}7804 \times 10^{-13}$	$4{,}6896 \times 10^{-13}$	$1{,}8812 \times 10^{-12}$	$1{,}3269 \times 10^{-12}$	$1{,}3216 \times 10^{-12}$
	0.2	$7{,}9048 \times 10^{-13}$	$4{,}281 \times 10^{-13}$	$4{,}0092 \times 10^{-12}$	$2{,}6219 \times 10^{-12}$	$1{,}7852 \times 10^{-12}$
	0.3	$6{,}6258 \times 10^{-13}$	$2{,}4691 \times 10^{-13}$	$5{,}6399 \times 10^{-12}$	$1{,}5723 \times 10^{-11}$	$1{,}3713 \times 10^{-12}$
	0.4	$2{,}0606 \times 10^{-12}$	$1{,}5969 \times 10^{-12}$	$5{,}6328 \times 10^{-12}$	$1{,}0759 \times 10^{-10}$	$6{,}3949 \times 10^{-14}$
$R(t)$	0.5	$4{,}496 \times 10^{-12}$	$4{,}0057 \times 10^{-12}$	$4{,}6434 \times 10^{-12}$	$5{,}1058 \times 10^{-10}$	$2{,}1405 \times 10^{-12}$
	0.6	$7{,}3666 \times 10^{-12}$	$6{,}9207 \times 10^{-12}$	$3{,}2667 \times 10^{-12}$	$1{,}8319 \times 10^{-9}$	$5{,}2456 \times 10^{-12}$
	0.7	$1{,}1273 \times 10^{-11}$	$1{,}1079 \times 10^{-11}$	$7{,}3186 \times 10^{-13}$	$5{,}3956 \times 10^{-9}$	$9{,}2442 \times 10^{-12}$
	0.8	$1{,}6692 \times 10^{-11}$	$1{,}7263 \times 10^{-11}$	$3{,}9275 \times 10^{-12}$	$1{,}3749 \times 10^{-8}$	$1{,}4126 \times 10^{-11}$
	0.9	$2{,}1956 \times 10^{-11}$	$2{,}4414 \times 10^{-11}$	$1{,}0187 \times 10^{-11}$	$3{,}137 \times 10^{-8}$	$1{,}9869 \times 10^{-11}$
	1	$2{,}6454 \times 10^{-11}$	$3{,}3054 \times 10^{-11}$	$1{,}9806 \times 10^{-11}$	$6{,}5602 \times 10^{-8}$	$2{,}6455 \times 10^{-11}$

of TWM, although CPM, LePM use lower degree polynomials. Therefore, CPM and LePM provide more accurate results than LaPM and TWM.

Example 2. In this example, in order to determine the initial conditions and the parameters, we use the reported Covid 19 data for April 4, 2020 released in [48] Since April 4, 2020 was the first reported day, after the first Covid 19 case was declared on March 11, 2020. Therefore, we regard the data on April 4, 2020 as the initial number of susceptible people, infected people, and removed people in Türkiye on April 4. The transmission rate is $\beta = 1/14$ ($1/days$) ~ 0.0714 and the rate of recovery can be determined as $\beta = 1287/23934 \sim 0.0538$ [48, 49]. Setting $L = 60$ for time interval [0,60] and considering the parameters and the initial conditions as listed in Table 4,

we obtain the Chebyshev polynomial solutions, Legendre polynomial solutions and Laguerre polynomial solutions given in Table 5.

We compare the approximate solutions for the susceptible population $S(t)$, the infected population $I(t)$, and the removed population $R(t)$, obtained by the Chebyshev polynomial method (CPM), Legendre polynomial method

Table 3. Comparison of the absolute residual errors of *CPM, LePM, LaPM* with *TWM* [26] [created by author]

ReS_N ReI_N ReR_N	t	CPM N = 9	LePM N = 9	LaPM N = 9	TWM [26] N = 10
	0	$4{,}0115 \times 10^{-17}$	$2{,}959 \times 10^{-16}$	$9{,}6194 \times 10^{-12}$	$3{,}8503 \times 10^{-13}$
	0.1	$2{,}2379 \times 10^{-15}$	$2{,}5741 \times 10^{-15}$	$1{,}0036 \times 10^{-11}$	$1{,}9731 \times 10^{-14}$
	0.2	$4{,}1725 \times 10^{-15}$	$3{,}8361 \times 10^{-15}$	$1{,}0439 \times 10^{-11}$	$3{,}9085 \times 10^{-15}$
	0.3	$3{,}2846 \times 10^{-15}$	$3{,}6212 \times 10^{-15}$	$1{,}0838 \times 10^{-11}$	$8{,}2499 \times 10^{-16}$
	0.4	$1{,}9158 \times 10^{-15}$	$1{,}5790 \times 10^{-15}$	$1{,}1257 \times 10^{-11}$	$1{,}2032 \times 10^{-15}$
ReS_N	0.5	$3{,}2545 \times 10^{-17}$	$3{,}0454 \times 10^{-16}$	$1{,}1657 \times 10^{-11}$	$3{,}7199 \times 10^{-17}$
	0.6	$2{,}9604 \times 10^{-15}$	$3{,}2978 \times 10^{-15}$	$1{,}2055 \times 10^{-11}$	$8{,}8818 \times 10^{-16}$
	0.7	$8{,}9046 \times 10^{-15}$	$8{,}5669 \times 10^{-15}$	$1{,}249 \times 10^{-11}$	$7{,}6465 \times 10^{-16}$
	0.8	$2{,}1966 \times 10^{-14}$	$2{,}2304 \times 10^{-14}$	$1{,}2885 \times 10^{-11}$	$3{,}9807 \times 10^{-15}$
	0.9	$4{,}9315 \times 10^{-14}$	$4{,}8976 \times 10^{-14}$	$1{,}3297 \times 10^{-11}$	$2{,}1719 \times 10^{-14}$
	1	$2{,}5164 \times 10^{-17}$	$3{,}1346 \times 10^{-16}$	$1{,}3502 \times 10^{-11}$	$3{,}8908 \times 10^{-13}$
	0	$7{,}0824 \times 10^{-17}$	$3{,}9542 \times 10^{-16}$	$1{,}404 \times 10^{-11}$	$4{,}1895 \times 10^{-13}$
	0.1	$1{,}1281 \times 10^{-14}$	$1{,}1747 \times 10^{-14}$	$1{,}3676 \times 10^{-11}$	$2{,}1857 \times 10^{-14}$
	0.2	$8{,}7951 \times 10^{-15}$	$8{,}3289 \times 10^{-15}$	$1{,}3293 \times 10^{-11}$	$5{,}6389 \times 10^{-15}$
	0.3	$5{,}3971 \times 10^{-15}$	$5{,}8635 \times 10^{-15}$	$1{,}2918 \times 10^{-11}$	$8{,}789 \times 10^{-16}$
	0.4	$2{,}8005 \times 10^{-15}$	$2{,}3339 \times 10^{-15}$	$1{,}2514 \times 10^{-11}$	$1{,}1439 \times 10^{-15}$
ReI_N	0.5	$6{,}1473 \times 10^{-17}$	$4{,}054 \times 10^{-16}$	$1{,}2137 \times 10^{-11}$	$1{,}0432 \times 10^{-15}$
	0.6	$3{,}7871 \times 10^{-15}$	$4{,}2543 \times 10^{-15}$	$1{,}1762 \times 10^{-11}$	$1{,}5831 \times 10^{-15}$
	0.7	$1{,}1075 \times 10^{-14}$	$1{,}0608 \times 10^{-14}$	$1{,}1341 \times 10^{-11}$	$2{,}2195 \times 10^{-16}$
	0.8	$2{,}6530 \times 10^{-14}$	$2{,}6998 \times 10^{-14}$	$1{,}0969 \times 10^{-11}$	$7{,}0158 \times 10^{-15}$
	0.9	$5{,}8417 \times 10^{-14}$	$5{,}7948 \times 10^{-14}$	$1{,}0578 \times 10^{-11}$	$1{,}7018 \times 10^{-14}$
	1	$5{,}4365 \times 10^{-17}$	$4{,}1484 \times 10^{-16}$	$1{,}0427 \times 10^{-11}$	$4{,}1454 \times 10^{-13}$
	0	$1{,}7476 \times 10^{-17}$	$3{,}0451 \times 10^{-17}$	$2{,}4210 \times 10^{-13}$	$1{,}5677 \times 10^{-17}$
	0.1	$9{,}0902 \times 10^{-15}$	$9{,}0424 \times 10^{-15}$	$1{,}8765 \times 10^{-13}$	$9{,}1722 \times 10^{-15}$
	0.2	$4{,}5764 \times 10^{-15}$	$4{,}624 \times 10^{-15}$	$1{,}6732 \times 10^{-13}$	$4{,}4901 \times 10^{-15}$
	0.3	$2{,}158 \times 10^{-15}$	$2{,}1105 \times 10^{-15}$	$1{,}4337 \times 10^{-13}$	$2{,}2490 \times 10^{-15}$
	0.4	$8{,}340 \times 10^{-16}$	$8{,}8730 \times 10^{-16}$	$1{,}297 \times 10^{-13}$	$7{,}5359 \times 10^{-16}$
ReR_N	0.5	$1{,}5104 \times 10^{-17}$	$3{,}2098 \times 10^{-17}$	$1{,}0634 \times 10^{-13}$	$1{,}1048 \times 10^{-16}$
	0.6	$8{,}7017 \times 10^{-16}$	$8{,}2311 \times 10^{-16}$	$8{,}2989 \times 10^{-14}$	$9{,}6009 \times 10^{-16}$
	0.7	$2{,}1277 \times 10^{-15}$	$2{,}1747 \times 10^{-15}$	$6{,}9314 \times 10^{-14}$	$2{,}0272 \times 10^{-15}$
	0.8	$4{,}6066 \times 10^{-15}$	$4{,}5598 \times 10^{-15}$	$4{,}5365 \times 10^{-14}$	$4{,}7073 \times 10^{-15}$
	0.9	$9{,}060 \times 10^{-15}$	$9{,}1066 \times 10^{-15}$	$2{,}5038 \times 10^{-14}$	$8{,}9866 \times 10^{-15}$
	1	$1{,}2750 \times 10^{-17}$	$3{,}3743 \times 10^{-17}$	$2{,}9412 \times 10^{-14}$	$5{,}4134 \times 10^{-16}$

Table 4. The initial conditions and the values of the parameters

Data	P	S_0	I_0	R_0	β	ν
Values	84,000,000	83,996,609	3013	378	0.0538	0.0714

(LePM) and Laguerre polynomial method (LaPM) with the Pell-Lucas collocation method (PLCM), recently studied in [29], and the Runge Kutta method (RK4) when the step size of the Runge-Kutta iteration is $\Delta t = 0.1$ in the interval [0,60] and the other numerical techniques use the fifth order polynomial approximation. As shown in Figure 1 that all the numerical techniques are in good agreement. Namely, the number of susceptible individuals, $S(t)$, decreases from

Table 5. The chebyshev polynomial solutions, the legendre polynomial solutions and the laguerre polynomial solutions

$S_5(t), I_5(t), R_5(t)$	a_n, b_n, c_n	$\phi_n(t)$		
		$\phi_n(t) = T_n(t)$ CPM	$\phi_n(t) = P_n(t)$ LePM	$\phi_n(t) = L_n(t)$ LaPM
$S_5(t) = \sum_{n=0}^{5} a_n\phi_n(t)$	a_0	8.3987×10^7	1.4886×10^8	1.4888×10^8
	a_1	-1.1350×10^4	-1.4127×10^4	-2.7951×10^2
	a_2	-1.4843×10^3	-2.4723×10^3	-5.0161
	a_3	-1.2999×10^2	-2.6018×10^2	0.0915
	a_4	-8.5362	-19.5631	-1.4277×10^{-3}
	a_5	-0.4477	-1.1399	4.4330×10^{-5}
$I_5(t) = \sum_{n=0}^{5} b_n\phi_n(t)$	b_0	5.4806×10^3	9.4974×10^3	5.4363×10^3
	b_1	2.8040×10^3	3.4901×10^3	-69.0802
	b_2	3.6642×10^2	6.1032×10^2	1.2391
	b_3	32.0404	64.1289	-2.2566×10^{-2}
	b_4	2.0974	4.8067	3.5248×10^{-4}
	b_5	0.1093	0.2783	-1.0825×10^{-5}
$R_5(t) = \sum_{n=0}^{5} c_n\phi_n(t)$	c_0	7.8976×10^3	1.3337×10^4	9.6234×10^2
	c_1	8.5457×10^3	1.0637×10^4	-2.1043×10^2
	c_2	1.1179×10^3	1.8620×10^3	3.7769
	c_3	97.9539	1.9605×10^2	-0.0689
	c_4	6.4389	14.7564	0.0011
	c_5	0.3383	0.8616	-3.3506×10^{-5}

83,996,609 to 83,973,800 individuals in 60-day time period when the number of infected individuals, $I(t)$, increases from 3013 to 8685 individuals and the number of removed individuals, $R(t)$, increases from 378 to 17619 individuals. Figure 2 also shows that the growth of the removed population $R(t)$ is slower than that of the infected population $I(t)$. This means that infected individuals spread the disease to susceptible individuals faster than the rate of recovery.

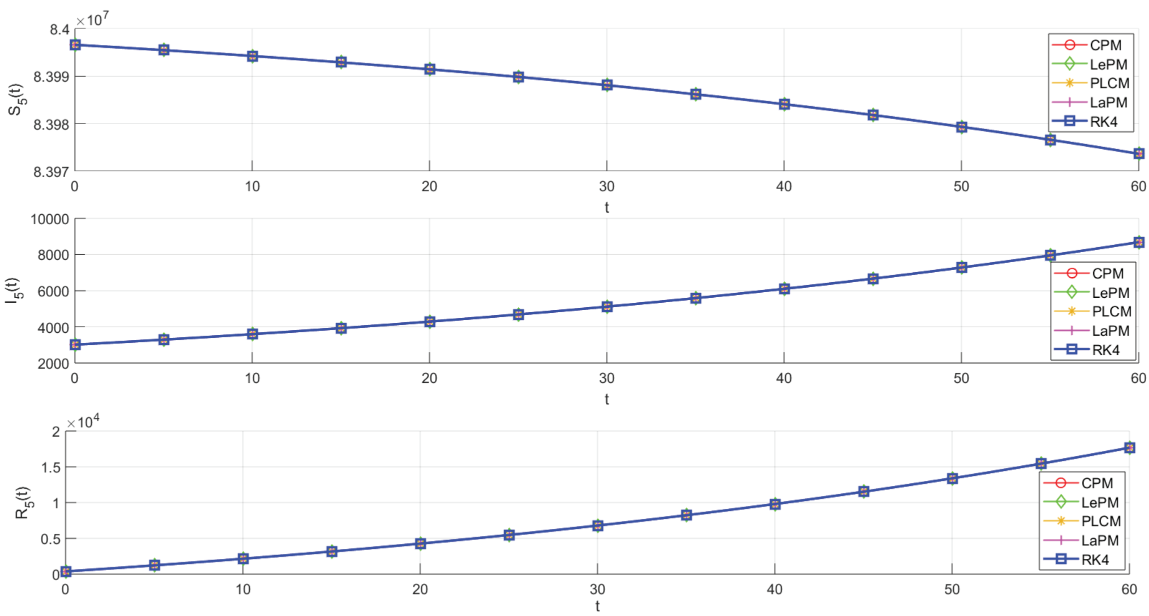

Figure 1. Comparison of $S_5(t)$, $I_5(t)$, $R_5(t)$, obtained by CPM, LePM, LaPM, PLCM [37] and RK4.

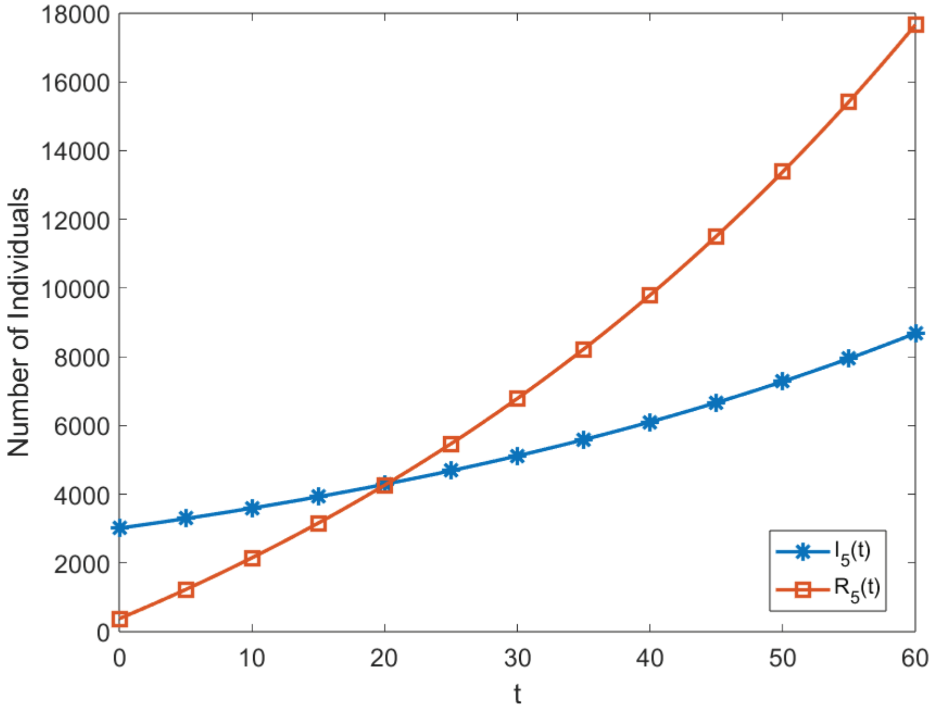

Figure 2. Comparison of the number of infected and removed people.

Table 6. Comparison of the absolute residual errors ReS_N, ReI_N and ReR_N, for $N = 8$

ReS_N ReI_N ReR_N	t	CPM	LePM	LaPM	PLCM [29]
	t=0	2.6445×10^{-14}	5.3620×10^{-15}	2.7274×10^{-14}	2.5055×10^{-5}
	t=10	1.5806×10^{-7}	1.5806×10^{-7}	1.5806×10^{-7}	3.9551×10^{-7}
	t=20	9.1073×10^{-8}	9.1073×10^{-8}	9.1073×10^{-8}	5.4811×10^{-8}
ReS_8	t=30	7.4352×10^{-8}	7.4352×10^{-8}	7.4352×10^{-8}	1.7356×10^{-14}
	t=40	9.0451×10^{-8}	9.0451×10^{-8}	9.0451×10^{-8}	2.7206×10^{-8}
	t=50	1.5590×10^{-7}	1.5590×10^{-7}	1.5590×10^{-7}	7.7954×10^{-8}
	t=60	2.9876×10^{-14}	6.9652×10^{-14}	7.7243×10^{-14}	8.1501×10^{-15}
	t=0	1.8899×10^{-14}	8.2465×10^{-15}	1.9978×10^{-14}	4.5783×10^{-6}
	t=10	2.9245×10^{-8}	2.9245×10^{-8}	2.9245×10^{-8}	7.1278×10^{-8}
	t=20	1.6621×10^{-8}	1.6621×10^{-8}	1.6621×10^{-8}	9.7302×10^{-9}
ReI_8	t=30	1.3369×10^{-8}	1.3369×10^{-8}	1.3369×10^{-8}	1.0093×10^{-13}
	t=40	1.6000×10^{-8}	1.6000×10^{-8}	1.6000×10^{-8}	4.6659×10^{-9}
	t=50	2.7087×10^{-8}	2.7087×10^{-8}	2.7087×10^{-8}	1.3106×10^{-8}
	t=60	2.4593×10^{-14}	2.9889×10^{-14}	5.2623×10^{-14}	3.4531×10^{-14}
	t=0	7.6999×10^{-15}	1.6644×10^{-14}	1.4656×10^{-14}	2.0477×10^{-5}
	t=10	1.2882×10^{-7}	1.2882×10^{-7}	1.2882×10^{-7}	3.2423×10^{-7}
	t=20	7.4452×10^{-8}	7.4452×10^{-8}	7.4452×10^{-8}	4.5081×10^{-8}
ReR_8	t=30	6.0984×10^{-8}	6.0984×10^{-8}	6.0984×10^{-8}	1.4048×10^{-14}
	t=40	7.4452×10^{-8}	7.4452×10^{-8}	7.4452×10^{-8}	2.2540×10^{-8}
	t=50	1.2882×10^{-7}	1.2882×10^{-7}	1.2882×10^{-7}	6.4847×10^{-8}
	t=60	1.4945×10^{-14}	3.2176×10^{-14}	1.0288×10^{-14}	2.9582×10^{-15}

For further comparison to check the efficiency and robustness of CPM, LePM and LaPM, we compute the residual errors of the approximate solutions of the susceptible population $S_N(t)$, the infected population $I_N(t)$ and the removed population $R_N(t)$ where the values of the transmission rate β, the recovery rate v and the total population size P are listed in Table 1. The residual errors obtained by CPM, LePM and LaPM when $N = 8$ and $N = 10$ are compared with the results of Yüzbaşı and Yıldırım [29] obtained by the Pell-Lucas collocation method (PLCM). Tables 6 and 7 present comparisons of the absolute residual errors ReS_N, ReI_N, ReR_N for $N = 8$ and $N = 10$ respectivelyy.

As observed in Table 6, when $N = 8$, CPM, LePM and LaPM yield similar residual errors to PLCM. For all these methods, Table 6 shows that the absolute residual errors ReS_N, ReI_N, ReR_N are not respectively larger than 10^{-7}, 10^{-8} and 10^{-7} for $t \in (0,60)$. As N increases to 10, one can observe in Table 7 that CPM, LePM and LaPM provide similar residual errors ReS_N, ReI_N, ReR_N with each other but better results than those of PLCM for $t \in (0,60)$. Furthermore, it

Table 7. Comparison of the absolute residual errors ReS_N, ReI_N and ReR_N, for $N = 10$

ReS_N ReI_N ReR_N	t	CPM	LePM	LaPM	PLCM [29]
	t=0	2.4008×10^{-14}	1.9308×10^{-15}	7.1148×10^{-15}	1.7821×10^{-8}
	t=10	6.4027×10^{-11}	6.3995×10^{-11}	6.4003×10^{-11}	1.0382×10^{-10}
	t=20	1.4426×10^{-14}	2.1246×10^{-14}	1.4180×10^{-15}	1.0065×10^{-11}
ReS_{10}	t=30	9.9959×10^{-12}	1.0035×10^{-11}	1.0004×10^{-11}	1.7963×10^{-14}
	t=40	7.1641×10^{-15}	3.6190×10^{-14}	3.2176×10^{-15}	5.4862×10^{-12}
	t=50	7.2742×10^{-11}	7.2692×10^{-11}	7.2738×10^{-11}	2.3212×10^{-11}
	t=60	1.3613×10^{-14}	4.6032×10^{-14}	5.4246×10^{-15}	6.2135×10^{-14}
	t=0	8.9461×10^{-15}	7.2896×10^{-15}	1.1666×10^{-14}	1.5858×10^{-8}
	t=10	6.6527×10^{-11}	6.6521×10^{-11}	6.6505×10^{-11}	9.2552×10^{-11}
	t=20	7.0923×10^{-15}	2.8868×10^{-16}	1.3670×10^{-16}	9.0502×10^{-12}
ReS_{10}	t=30	1.0370×10^{-11}	1.0379×10^{-11}	1.0379×10^{-11}	5.9179×10^{-14}
	t=40	3.2403×10^{-16}	8.6190×10^{-15}	1.6738×10^{-14}	4.9293×10^{-12}
	t=50	7.5241×10^{-11}	7.5231×10^{-11}	7.5225×10^{-11}	2.1138×10^{-11}
	t=60	7.1142×10^{-15}	1.8055×10^{-14}	2.1556×10^{-14}	3.2251×10^{-14}
	t=0	4.7398×10^{-14}	8.5106×10^{-15}	4.9137×10^{-15}	1.9418×10^{-9}
	t=10	2.4690×10^{-12}	2.5211×10^{-12}	2.5037×10^{-12}	1.1024×10^{-11}
	t=20	3.6205×10^{-14}	1.1633×10^{-14}	9.5127×10^{-15}	1.0284×10^{-12}
ReS_{10}	t=30	4.0023×10^{-13}	3.5641×10^{-13}	3.8113×10^{-13}	5.2996×10^{-14}
	t=40	2.8236×10^{-14}	1.2199×10^{-14}	1.5713×10^{-14}	5.4701×10^{-13}
	t=50	2.4841×10^{-12}	2.5219×10^{-12}	2.4914×10^{-12}	2.2316×10^{-12}
	t=60	2.6602×10^{-14}	9.1213×10^{-15}	2.3371×10^{-15}	4.9546×10^{-14}

Table 8. Comparison of the maximum absolute residual errors $maxReS_N$, $maxReI_N$ and $maxReR_N$, for $t \in [0,60]$

$maxReS_N$ $maxReI_N$ $maxReR_N$	N	CPM	LePM	LaPM	PLCM [29]
$maxReS_8$		1.1153×10^{-6}	1.1153×10^{-6}	1.1153×10^{-6}	2.5055×10^{-5}
$maxReI_8$	N = 8	2.0827×10^{-7}	2.0827×10^{-7}	2.0827×10^{-7}	4.5783×10^{-6}
$maxReR_8$		9.0698×10^{-7}	9.0698×10^{-7}	9.0698×10^{-7}	2.0477×10^{-5}
$maxReS_{10}$		5.3986×10^{-10}	5.3990×10^{-10}	5.3977×10^{-10}	1.7821×10^{-8}
$maxReI_{10}$	N = 10	5.5796×10^{-10}	5.5785×10^{-10}	5.5793×10^{-10}	1.5858×10^{-8}
$maxReR_{10}$		1.8151×10^{-11}	1.8118×10^{-11}	1.8153×10^{-11}	1.9418×10^{-9}

is clear from Table 8 that for N increases to $N = 10$, these residual errors have maximum values which are not larger than 10^{-10}. Therefore, one can say that CPM, LePM, and LaPM are as efficient as PLCM for low-degree polynomials but provide more accurate results than PLCM as the degree of the polynomial is increased.

CONCLUSION

The major contribution of this paper can be considered as the approximate solutions for solving the Susceptible-Infected-Removed model of the Covid 19 spread. These approximate solutions are obtained by the use of orthogonal Chebyshev, Legendre, and Laguerre polynomials. The obtained approximate solutions are compared with the other numerical results in figures and tables and the accuracy of the method is examined through the absolute and residual errors. We observe that these polynomials they are all effective in reducing the difficulty of solving systems of nonlinear ordinary differential equations and are easy to implement with low computational cost because discretization of the domain is not required. Furthermore, Chebyshev, Legendre and Laguerre polynomials provide more accurate results than other numerical techniques in the literature. As we compare these polynomials with each other, Chebyshev polynomials and Legendre polynomials provide more accurate results than Laguerre polynomials for the time interval [0,1], but when we extend it to a larger interval, the Laguerre polynomials are as efficient as Chebyshev and Legendre polynomials.

It is worth mentioning that many factors come into play in order to obtain accurate results for realistic problems. In addition to efficiency of the technique used, the model should be well established for good accuracy and the problem parameters should be well estimated in along with the given data. Moreover, the data should be reliable and realistic so that the obtained results can reflect the reality. In this sense, the Susceptible-Infected-Removed model is preferred due to its basic structure to examine the efficiency of the method. Whenever a numerical approach, applied on SIR model, results in accurate solutions, then it can be adopted to solve more comprehensive epidemic models. The method, in this paper, based on the use of orthogonal Chebyshev, Legendre, and Laguerre polynomials can be applied to extensions of the SIR model. Especially, the epidemic models that include births and natural deaths, the infection rate of the exposed population and, the influence of factors such as vaccination or immunity can be addressed as future investigations.

NOMENCLATURE

S	Susceptible population
I	Infected population
R	Removed population
P	Total population
β	Rate of transmission from susceptible individuals to infected individuals
v	Recovery rate
t	Time variable
S_0	The initial number of susceptible individuals
I_0	The initial number of infected individuals
R_0	The initial number of removed individuals
CPM	Chebyshev polynomials method
LePM	Legendre polynomials method
LaPM	Laguerre polynomials method
TWM	Taylor wavelets method
LaWM	Laguerre wavelets method
PLCM	Pell-Lucas Collocation method

DATA AVAILABILITY STATEMENT

The data about the Covid-19 disease to determine the initial conditions and some of the parameters are available as open data in the General Coronavirus Table on the website of Turkish Ministry of Health: https://covid19.saglik.gov.tr/TR-66935/genelkoronavirus-tablosu.html

CONFLICT OF INTEREST

The author declared no potential conflicts of interest with respect to the research, authorship, and/or publication of this article.

ETHICS

There are no ethical issues with the publication of this manuscript.

STATEMENT ON THE USE OF ARTIFICIAL INTELLIGENCE

Artificial intelligence was not used in the preparation of the article.

REFERENCES

[1] Sampath S, Khedr A, Qamar S, Tekin A, Singh R, Green R, et al. Pandemics throughout the history. Cureus 2021;13:e18136. [CrossRef]

[2] Akin L, Gözel MG. Understanding dynamics of pandemics. Turk J Med Sci 2020;50:515–519. [CrossRef]

[3] Taylor CA, Boulos C, Memoli MJ. The 1968 influenza pandemic and COVID-19 outcomes. medRxiv 2022;2022:1-15. [CrossRef]

[4] Record NR, Pershing A. A note on the effects of epidemic forecasts on epidemic dynamics. PeerJ 2020;8:e9649. [CrossRef]

[5] Özbek L. A study on the estimation of COVID-19 cases with the adaptive Kalman filter (AKF). Sigma J Eng Nat Sci 2022;40:323–343.

[6] Mohajan HK. Mathematical analysis of SIR model for COVID-19 transmission. J Innov Med Res 2022;1:1–18. [CrossRef]

[7] Kalachev L, Graham J, Landguth EL. A simple modification to the classical SIR model to estimate the proportion of under-reported infections. Infect Dis Model 2024;9:1147–1162. [CrossRef]

[8] Jayatilaka R, Patel R, Brar M, Tang Y, Jisrawi NM, Chishtie F, et al. A mathematical model of COVID-19 transmission. Mater Today Proceed 2022;54:101–112. [CrossRef]

[9] Cooper I, Mondal A, Antonopoulos CG. A SIR model assumption for the spread of COVID-19 in different communities. Chaos Solit Fract 2020;139:110057. [CrossRef]

[10] Muñoz-Fernández GA, Seoane JM, Seoane-Sepúlveda JB. A SIR-type model describing the successive waves of COVID-19. Chaos Solit Fract 2021;144:110682. [CrossRef]

[11] Mostak A, Khan MHOR, Sarker MA. COVID-19 SIR model: Bifurcation analysis and optimal control. Results Control Optim 2023;12:100246. [CrossRef]

[12] Cooper I, Mondal A, Antonopoulos CG, Mishra A. Dynamical analysis of the infection status in diverse communities using a modified SIR model. Nonlinear Dyn 2022;109:19–32. [CrossRef]

[13] Zhang H, Madhusudanan V, Murthy BSN, Srinivas MN. Fuzzy analysis of SVIRS disease system with Holling type-II saturated incidence rate. Math Problems Eng 2022;2022:1330875. [CrossRef]

[14] Kalyan D, Srinivas MN, Shahrear P, Rahman SMS, Nahid MH, Murthy BSN. Transmission dynamics and control of COVID-19. J App Nonlinear Dyn 2023;12:405-425. [CrossRef]

[15] Shahrear P, Rahman SMS, Nahid MH. Prediction and mathematical analysis of COVID-19 outbreak in Bangladesh. Results Appl Math 2021;10:100145. [CrossRef]

[16] Sweatha S, Monisha P, Sindu Devi S. An SIR model for COVID-19 outbreak in India. Commun Math Appl 2022;13:661–669. [CrossRef]

[17] Youssef IK, Hassan MHM. A comparative study of mathematical models of epidemic diseases. Appl Sci 2022;12:12639. [CrossRef]

[18] Gümüş ÖA, Selvam AGM, Kilinç N, Janagaraj R. Analyses of the SIR epidemic model including treatment and immigration. J Math Sci Model 2024;7:1–13. [CrossRef]

[19] Alshammari FS, Akyıldız FT. Global stability for complicated SIR epidemic models. J Funct Spaces 2021;2021:5207152. [CrossRef]

[20] Türkyilmazoğlu M. Solutions to SIR/SEIR epidemic models with exponential series. Comput Biol Med 2024;183:109294. [CrossRef]

[21] Prodanov D. Computational aspects of approximate analytic solutions of the SIR model. Nonlinear Dyn 2023;111:15613–15631. [CrossRef]

[22] Barlow NS, Weinstein SJ. Accurate closed-form solution of the SIR epidemic model. Physica D 2020;408:132540. [CrossRef]

[23] Hasan S, Al-Zoubi A, Freihet A, Al-Smadi M, Momani S. Solution of fractional SIR epidemic model using residual power series method. Appl Math Inform Sci 2019;13:153–161. [CrossRef]

[24] Secer A, Ozdemir N, Bayram M. A Hermite polynomial approach for solving the SIR model of epidemics. Mathematics 2018;6:305. [CrossRef]

[25] Ucar D, Çelik E. Analysis of COVID-19 disease with SIR model and Taylor matrix method. AIMS Math 2022;7:11188–11200. [CrossRef]

[26] Vivek MK. Spreading behavior of biological SIR system using Taylor wavelet method. Results Control Optim 2023;13:100316. [CrossRef]

[27] Shiralashetti S, Kumbinarasaiah S. Laguerre wavelets exact Parseval frame-based numerical method. Int J Appl Math 2020;6:101–112. [CrossRef]

[28] Özdek D. Chebyshev polynomial solution for the SIR model of COVID-19. Gazi J Eng Sci 2023;9:39–47. [CrossRef]

[29] Yüzbaşı Ş, Yıldırım G. A Pell-Lucas collocation approach for an SIR model. Mathematics 2023;11:697. [CrossRef]

[30] Ozaltun Simsek G, Beler A, Gümgüm S. Gegenbauer wavelet solutions of the SIR and SITR systems. Int J Biomath 2024;17:1–20. [CrossRef]

[31] Szegö G. Orthogonal polynomials. Rhode Island: American Mathematical Society; 1939.

[32] Arfken GB, Weber HJ. Mathematical methods for physicists. London: Elsevier Academic Press; 2005.

[33] Kreyszig E. Introductory functional analysis with applications. London: Wiley; 1978.

[34] Gümgüm S, Özdek D, Özaltun G. Legendre wavelet solution of high order nonlinear ordinary delay differential equations. Turk J Math 2019;43:1339–1352. [CrossRef]

[35] Gümgüm S, Özdek D, Özaltun G, Bildik N. Legendre wavelet solution of neutral differential equations with proportional delays. J Appl Math Comput 2019;61:389–404. [CrossRef]

[36] Mason JC, Handscomb DC. Chebyshev polynomials. Boca Raton: Chapman & Hall/CRC; 2003. [CrossRef]

[37] Rivlin TJ. Chebyshev polynomials: From approximation theory to algebra and number theory. 2nd ed. New York: Wiley; 1990.

[38] Lima FMS. Lecture notes on Legendre polynomials: Their origin and main properties. arXiv preprint 2022;2022:1–15. doi: 10.48550/arXiv.2210.10942

[39] Yüzbaşı Ş, Yıldırım G. Laguerre collocation method for solutions of systems of first order linear differential equations. Turk J Math Comput Sci 2018;10:222–241.

[40] Elahi Z, Akram G, Siddiqi SS. Laguerre approach for solving system of linear Fredholm integro-differential equations. Math Sci 2018;12:185–195. [CrossRef]

[41] Beler A, Özaltun Şimşek G, Gümgüm S. Numerical solutions of the HIV infection model of CD4(+) cells by Laguerre wavelets. Math Comput Simul 2023;209:205–219. [CrossRef]

[42] Paul SK, Mishra LN, Mishra VN, Baleanu D. An effective method for solving nonlinear integral equations involving the Riemann–Liouville fractional operator. AIMS Math 2023;8:17448–17469. [CrossRef]

[43] Paul SK, Mishra LN, Mishra VN. Approximate numerical solutions of fractional integral equations using Laguerre and Touchard polynomials. Palestine J Math 2023;12:416-431.

[44] Kreiss A, Van Keilegom I. Semi-parametric estimation of incubation and generation times by means of Laguerre polynomials. J Nonparametric Stat 2022;34:570–606. [CrossRef]

[45] Ahmadi MR, Adibi H. The Chebyshev tau technique for the solution of Laplace's equation. Appl Math Comput 2007;184:895–900. [CrossRef]

[46] Ibraheem GH, Al-Jawary MA. The operational matrix of Legendre polynomials for solving thin film flow problems. Alexandria Eng J 2020;59:4027–4033. [CrossRef]

[47] Baishya C, Veeresha P. Laguerre polynomial-based operational matrix of integration for solving fractional differential equations with non-singular kernel. Proceed Royal Soc A 2021;477:20210438. [CrossRef]

[48] Türkiye Ministry of Health. COVID-19 information platform. Ankara: Ministry of Health; 2024.

[49] Ngonghala CN, Iboi E, Eikenberry S, Scotch M, MacIntyre CR, Bonds HM, et al. Mathematical assessment of the impact of non-pharmaceutical interventions on COVID-19. Math Biosci 2020;325:108364. [CrossRef]